

Stable Oscillations of Black Hole Accretion Discs

By MICHAEL A. NOWAK¹ AND D. E. LEHR²

¹JILA, Campus Box 440, Boulder, CO 80309-0440, USA

²Department of Physics, Stanford University, Stanford, CA 94305-0460, USA

The study of stable accretion disc oscillations relevant to black hole candidate (BHC) systems dates back over twenty years. Prior work has focused on both unstable and (potentially) stable disc oscillations. The former has often been suspected of being the underlying cause for the observed broad-band variability in BHC, whereas the latter has had little observational motivation until quite recently. In this article, we review both the observations and theory of (predominantly) stable oscillations in BHC systems. We discuss how variability, both broad-band and quasi-periodic, is characterized in BHC. We review previous claims of low frequency features in BHC, and we discuss the recent observational evidence for stable, high frequency oscillations in so-called ‘galactic microquasars’. As a potential explanation for the latter observations, we concentrate on a class of theories— with a rich history of study— that we call ‘diskoseismology’. We also discuss other recent alternative theories, namely Lense-Thirring precession of tilted rings near the disc inner edge. We discuss the advantages and disadvantages of each of these theories, and discuss possible future directions for study.

1. Overview of Black Hole States

Galactic X-ray sources are typically identified as black hole candidates (BHC) if they have measured mass functions indicating a compact object with $M \gtrsim 3 M_{\odot}$, or if their high energy spectra ($\sim 1 \text{ keV} - 10 \text{ MeV}$) and temporal variability ($\sim 10^{-3} - 10^2 \text{ Hz}$) are similar to other BHC. A review of the general observations, a number of theoretical models, plus individual descriptions of approximately twenty galactic BHC can be found in Tanaka & Lewin (1995). A review of the timing analyses can be found in van der Klis (1994) and van der Klis (1995). (These latter reviews attempt to link the energy spectra and timing observations, and they draw analogies to similar observations of neutron stars in low mass X-ray binaries.) A review of a subset of BHC with reasonably well-determined mass functions can be found in Nowak (1995).

The energy spectra of BHC have been historically labelled based upon observations of the soft X-ray band ($\sim 2 - 10 \text{ keV}$). Intense, quasi-thermal flux is referred to as the “high” state. Non-thermal flux in this band, typically a power law with a photon index[†] of ~ 1.7 , indicates that the BHC is in the “off” state (for extremely low intensity flux) or “low” state (for moderate intensity flux). The high state tends to have little variability, with a root mean square (rms) variability (cf. §2) of a few percent, whereas the low state tends to have an rms variability of several tens of percent. If a black hole candidate has a quasi-thermal soft X-ray component and significant high energy emission— occasionally modeled as a power law with a photon index ~ 2.5 — it is said to be in the “very high” state [cf. Miyamoto, et al. (1991)]. The rms variability of the very high state tends to be greater than that of the high state, but less than that of the low state [cf. Miyamoto, et al. (1992), Miyamoto, et al. (1993)]. Note that the labels “off”, “low”, “high”, and “very high” are purely qualitative in nature, but historically have been in popular use. No universally agreed upon quantitative definition for these

[†] Photon index here and throughout shall refer to the photon count rate, such that photon index Γ implies $\# \text{ photons/keV/s/cm}^2 \propto E^{-\Gamma}$, where E is the photon energy.

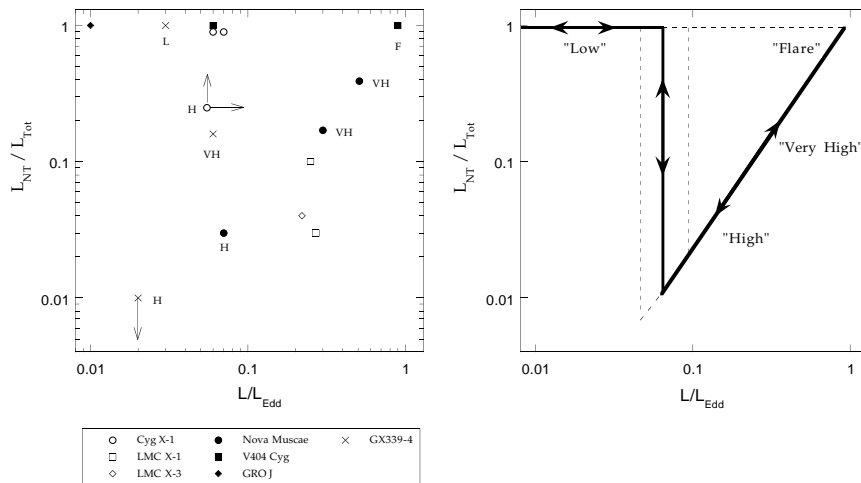


FIGURE 1. *Left:* The ratio of luminosity in a power law tail to total luminosity ($L_{\text{NT}}/L_{\text{Tot}}$) versus the ratio of total luminosity to Eddington luminosity (L/L_{Edd}) for black holes with well-determined mass functions. (Note: error bars are *not* plotted.) *Right:* Hypothetical evolutionary tracks for changes in BHC luminosity. [Figure adapted from Nowak (1995).]

states exist. More recently, the terms “hard state” and “soft state” have begun to be used in place of “low state” and “high/very high state”, respectively.

Figure 1 depicts this state behavior for several BHC with reasonably well-determined mass functions [cf. Nowak (1995)]. This figure shows the fraction of total luminosity in a power law-like tail as a function of the BHC’s fractional Eddington luminosity. BHC tend to be dominated by a power law tail for luminosities below $\sim 10\% L_{\text{Edd}}$, be completely dominated by a quasi-thermal, disc-like component near $\sim 10\% L_{\text{Edd}}$, and then begin to show a power law-like tail for $L \gtrsim 10\% L_{\text{Edd}}$. Above $10\% L_{\text{Edd}}$, the fraction of total luminosity in this power law tail (which typically has photon index $\Gamma \sim 2.5$) tends to increase with fractional Eddington luminosity. There are, of course, exceptions to the trends shown in Fig. 1; however, some transient BHC, such as Nova Muscae, have followed this trend very closely [cf. Miyamoto, et al. (1994)]. Historically, the soft flux component has been associated with a “classical” accretion disc, as discussed by Shakura & Sunyaev (1973).

2. Measuring Variability

The states of BHC have been further distinguished by their variability behavior, as discussed by van der Klis (1994), van der Klis (1995), Miyamoto, et al. (1992), and Miyamoto, et al. (1993). As shown in Figure 2, the greater the fraction of luminosity in a hard tail, the greater the amplitude of the observed variability. Miyamoto, et al. (1992) and Miyamoto, et al. (1993) further point out that states appear to have “canonical” variability behaviour not only in terms of amplitude, but also in terms of frequency distribution. This frequency distribution is typically described via Fourier transform techniques [cf. van der Klis (1994)], which we briefly describe below.

The key assumption in applying Fourier transform techniques is the assumption that the lightcurve represents a statistically stationary process [cf. Davenport & Root (1987)]. Effectively, this means that one assumes that individual data segments from the lightcurve are a good representation of an ensemble of *statistically* identical lightcurves. It is from

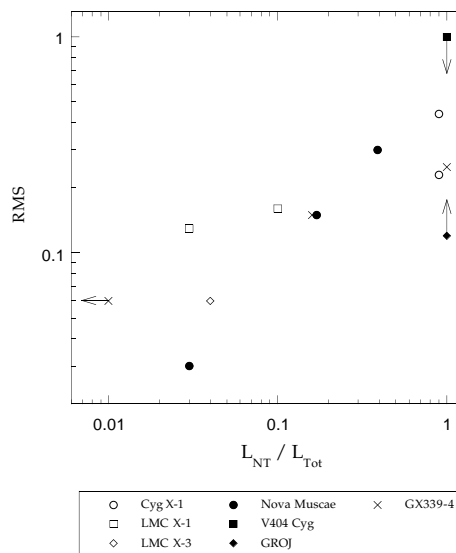


FIGURE 2. RMS variability versus ratio of luminosity in a power law tail to total luminosity (cf. Fig. 1). (Consistent energy bandpasses were not used for all depicted data points, although they predominantly represent a $\sim 2 - 35$ keV bandpass. Again, error bars are *not* plotted.) [Figure adapted from Nowak (1995).]

these individual lightcurve segments that one forms the power spectral density (PSD) [cf. van der Klis (1994)].

The PSD is calculated by dividing the lightcurve into segments of equal length and then taking a Fast Fourier Transform (FFT, i.e. discrete transform, cf. Press, et al. 1992) of each data segment. The squared amplitude of each individual FFT is then averaged together. Often one also averages over Fourier frequency bins. (Typically one chooses a scheme such that the number of frequency bins averaged over is $\propto f$, where f is the Fourier frequency.) This yields the resulting PSD for each lightcurve.

There are a number of different possible normalizations for the PSD; however, in this work we shall only refer to the normalization of Miyamoto, et al. (1992). For this normalization, the integral of the PSD over positive Fourier frequency yields the *square* of the total *root mean square (rms) amplitude* of the variability [Miyamoto, et al. (1992)]. That is, the PSD integrated over positive frequency yields $(\langle x^2 \rangle - \langle x \rangle^2) / \langle x \rangle^2$, where x is the photon count rate [cf. Miyamoto, et al. (1992), Miyamoto, et al. (1993)]. The rms can be calculated over specific Fourier frequency and energy spectral bandpasses. For a given narrow Fourier frequency interval, the rms is (to within a factor of $\sqrt{2}$) the fractional amount by which the lightcurve is sinusoidally modulated in that given Fourier frequency interval.

It is this measure of rms variability, typically calculated over frequency intervals of $\sim 10^{-3} - 10^2$ Hz in BHC, that leads to the characterization of power law tail-dominated sources (i.e. low and very high state sources) as being the most variable BHC. As a function of Fourier frequency, the PSD of all states can usually be described by (possibly multiple) broken power laws. However, occasionally superimposed on top of this broad band variability are narrow— compared to the the broad band PSD— features which are referred to as quasi-periodic oscillations (QPO). The properties of these features are the focus of the next section.

3. Quasi-periodic Variability observed in BHC

A quasi-periodic oscillation is usually taken to be *any* feature in the PSD that is well-fit by a Lorentzian of the form:

$$PSD(f) = \frac{R^2 Q f_{QPO}}{\pi \left[Q^2 (f_{QPO} - f)^2 + f_{QPO}^2 \right]} . \quad (3.1)$$

As written in eq. 3.1, this functional fit is relevant to the normalization of Miyamoto, et al. (1992). In the above, R is the fractional rms, f_{QPO} is the QPO frequency, and Q is the mode ‘quality factor’. If Δf_{QPO} is the full-width half maximum of the QPO feature, then $Q \approx f_{QPO}/\Delta f_{QPO}$.

For $Q \lesssim 3$, it is difficult to attribute the QPO to a discrete feature, as opposed to being merely an extension of the broad-band variability. For $Q \gtrsim 10$, the QPO is usually quite apparent in the PSD, and may be attributable to a discrete process in the BHC system. The question then arises of whether or not such a QPO feature represents a quasi-stable mode in an accretion disc. If the QPO feature is attributable to a mode or set of modes, then there are many possible mechanisms for generating a finite feature width in the PSD [cf. van der Klis (1994)]. Among these possibilities are: multiple modes distributed over frequencies $f_{QPO} \pm \Delta f_{QPO}$, a driven-damped mode with damping time scale $\tau_D \approx Q f_{QPO}^{-1}$, a mode that executes a random walk in phase of $\sim 2\pi$ on time scales of order τ_D , etc. Rarely does one have the statistics to determine which of these processes is responsible for the Q of the QPO.

Prior to the launch of the *Rossi X-ray Timing Explorer (RXTE)*, observations of QPO in BHC were made with *Ginga*, *BATSE*, and *Granat/SIGMA*. All of these observed QPO were at frequencies $\lesssim 10$ Hz, although the above instruments were for the most part limited to $\lesssim 60$ Hz. In addition, the rms variability of these features were all $\lesssim 10\%$, with $Q \lesssim \mathcal{O}(10)$. Below, we review some of the historical observations of black hole QPO.

3.1. Historical Observations

Reviews of some of the observed QPO features in BHC can be found in Nowak (1995) and Tanaka & Lewin (1995). Here we consider separately low state and high/very high state observations of BHC .

In the low state, Cygnus X-1 has shown QPO with rms as high as 15% [cf. Kouveliotou, et al. (1992a), Ubertini, et al. (1994), Vikhlinin, et al. (1994)]. The features were seen to have frequencies ~ 0.04 and 0.07 Hz. However, they appeared more as broad peaks in the otherwise broken power law PSD, and did not appear as discrete, narrow features. Similar features, with frequencies 0.04 and 0.2 Hz were seen in the hard state of the X-ray transient GRO J0422+32 (a.k.a. Nova Persei) [Kouveliotou, et al. (1992b), Sunyaev, et al. (1992), Sunyaev, et al. (1993)].

The source GX 339-4, which has been observed to transit through soft and hard X-ray states, has shown a relatively narrow [$Q \sim \mathcal{O}(10)$] QPO at 0.8 Hz [Grebenev, et al. (1991)] during its hard state. On the other hand, in its very high state GX 339-4 has also shown a narrow QPO at 6 Hz [Miyamoto, et al. (1991)]. Similar to this feature, the X-ray transient Nova Muscae has shown QPO in the range $3 - 8$ Hz during its very high state [Kitamoto, et al. (1992)].

In the soft state of LMC X-1 (which is the only state that has been observed in this source), there has been a claim of a 0.08 Hz feature with rms $\sim 4\%$ [Ebisawa, Mitsuda, & Inoue (1989)]. However, the count rates for these observations were extremely low, and it is unclear whether or not the putative variability detections described by Ebisawa, Mitsuda, & Inoue (1989) were below the effective Poisson noise limit. More recently,

Cui et al. (1997) has found evidence (based upon *RXTE* observations) of a 3 – 12 Hz feature in the soft state of Cygnus X–1. We note, however, that this feature is very broad and is difficult to associate with a discrete feature distinct from the observed broad-band variability.

Prior to the recent *RXTE* observations, a fairly clean division of QPO frequencies occurs if one ignores the 0.08 Hz QPO attributed to LMC X–1. Low frequency QPO ($\lesssim 1$ Hz) are seen in low/hard states, while high frequency QPO (~ 6 Hz) are seen in very high/soft states. Again, two questions arise. First, are these QPO associated with modes distinct from the broad-band variability? Second, if the QPO are distinct modes, are they associated with an accretion disc or with another component (such as a corona) in the BHC system? In the next subsection, we discuss a set of observed features in two BHC that may indeed be attributable to an accretion disc.

3.2. QPO in ‘Microquasars’

Recently, two rather unusual and dramatic X-ray transient galactic BHC have been observed: GRS 1915+105 [Mirabel & Rodriguez (1994), Morgan, Remillard, & Greiner (1997), Chen, Swank, & Taam (1997), Taam, Chen, & Swank (1997)] and GRO J1655-40 [Hjellming & Rupen (1995), Remillard et al. (1997)]. These sources were unusual in that they showed powerful, highly relativistic radio jets [Mirabel & Rodriguez (1994), Hjellming & Rupen (1995)]; hence, they have been dubbed ‘microquasars’. Furthermore, both have shown dramatic X-ray variability.

As observed by *RXTE*, GRS 1915+105 has shown X-ray count rates up to 10^5 cts/sec, which, given a distance of $\gtrsim 12$ kpc [Mirabel & Rodriguez (1994)], indicates a peak luminosity of over 10^{40} erg/s [Morgan, Remillard, & Greiner (1997), Chen, Taam, & Swank (1997)]. As discussed in Morgan, Remillard, & Greiner (1997), GRS 1915+105 has also shown intense variability patterns, with the luminosity changing by factors of several in only a few seconds. Amidst this spectral behavior, a host of different QPO features have been observed, ranging in frequencies from $\sim 0.1 - 10$ Hz [Morgan, Remillard, & Greiner (1987), Chen, Swank, & Taam (1997), Taam, Chen, & Swank (1997)]. Many of these QPOs have multiple harmonics, and both correlations and anti-correlations with source luminosity have been observed.

However, among the various QPO features seen, a high frequency QPO at 67 Hz has stood out because it apparently does not appreciably vary in frequency [Morgan, Remillard, & Greiner (1997)]. During the first epoch that this QPO feature was observed, it was relatively narrow ($Q \sim 20$), weak (rms variability $\sim 0.3 - 1.6\%$), and varied in frequency by $< 3\%$, despite factors of ~ 2 variations in source luminosity. When viewed in restricted bandpasses the rms variability was seen to increase with energy, with a maximum rms variability $\sim 6\%$ in the highest energy bandpass ($\sim 10 - 20$ keV). During subsequent observations similar features were observed, always at 67 ± 2 Hz [even on occasions when no soft, excess flux above a power law tail was observed in the spectrum; Morgan 1997, Private Communication].

A high frequency QPO feature has also been observed in GRO J1655-40, with frequency 300 Hz [Remillard, et al. (1997)]. However, this QPO was only detected once, and then only by summing several, individual observations. It was therefore difficult to place limits on the stability of this feature’s frequency. Like the 67 Hz feature in GRS 1915+105, this feature was weak (rms variability $\sim 0.8\%$). Furthermore, it was detectable only in the “hardest” spectra ($\sim 10 - 20$ keV). The 300 Hz feature in GRO J1655-40 was somewhat broader than the 67 Hz feature in GRS 1915+105. It is also notable in that a very accurate mass determination, $7 \pm 0.2 M_{\odot}$, has been made for the compact object in GRO J1655-40 [Orosz & Bailyn (1997)].

As we will discuss in §5, a number of properties displayed by these features, especially the 67 Hz feature in GRS 1915+105, are what one expects for stable, global oscillations of accretion discs. We will concentrate on theories of the oscillation of the innermost disc regions as potential explanations of these observations.

3.3. QPO in Active Galactic Nuclei

As discussed in §4, the characteristic time scales are one hundred thousand to one hundred million times longer in Active Galactic Nuclei (AGN) as compared to galactic BHC. Thus, if a 0.1 s QPO period is typical of a galactic black hole, then we might expect a 3 hour to year-long period to be typical for AGN. Such long time scales are very difficult for current missions to detect, as the shorter period is on the order of the *total* duration of a typical observation, and the longer period requires many dedicated observations. However, one AGN, IRAS18325–5926, has shown strong evidence for a 5.5×10^4 s periodicity that was observed for 9 cycles [Iwasawa, et al. (1998)]. Over these few cycles, there was no evidence for any strong change in phase, and the amplitude of the modulations was on the order of 10%. This is a somewhat stronger amplitude than observed for the 67 Hz and 300 Hz features described above, and therefore are difficult to explain with the models described in §5. Further (longer) observations are required to determine to what extent this AGN QPO is or is not similar to the QPO seen in the microquasars.

4. Characteristic Accretion Disc Frequencies and Time Scales

The fact that the 67 Hz QPO feature seen in GRS 1915+105 does not appear to vary in frequency as a function of luminosity suggests that this feature is tied to a fundamental frequency or time scale in the BHC system. As this frequency is apparently independent of accretion rate (i.e. luminosity), the relevant time scales are likely to be gravitational ones. The two most important parameters for the gravitational time scales of BHC are the black hole mass, M , and the angular momentum, J . We shall usually normalize the black hole mass to a solar mass. We will characterize the black hole angular momentum by the dimensionless parameter $a \equiv cJ/GM^2$, where c is the speed of light and G is the gravitational constant. For a Schwarzschild black hole, $a = 0$, while for a Kerr hole $a < 1$. Below we discuss the frequencies most relevant to orbits near the equatorial plane of a (possibly spinning) black hole. These frequencies are those most relevant to a thin accretion disc[†].

In what follows, we shall set $c = G = 1$. Furthermore, physical length scales will be normalized to GM/c^2 (≈ 15 km for $M = 10 M_\odot$), and frequencies will be normalized to c^3/GM ($\approx 3.2 \times 10^3$ Hz for $M = 10 M_\odot$). In general, characteristic gravitational length scales increase linearly with M , whereas characteristic time scales decrease linearly with M . Therefore, whereas 1 ms may be a relevant time scale for a galactic black hole, days or months might be the relevant time scale for a massive black hole at the center of an AGN. There will be four main frequencies of concern to us, each a function of radius r : the Keplerian (i.e. orbital) frequency, the radial epicyclic frequency, the vertical epicyclic frequency, and the Lense-Thirring precession frequency. We describe each of these in turn below.

The Keplerian frequency is the frequency with which a free particle azimuthally orbits

[†] We define the equatorial plane to be the plane perpendicular to the black hole angular momentum axis that passes through the center of the black hole. We shall consider a cylindrical coordinate system (r, ϕ, z) set up on this plane, with $z = 0$ being in the plane.

the black hole. This frequency, to a viewer observing at infinity, is given by:

$$\Omega = \left(r^{3/2} + a \right)^{-1} \quad (4.2)$$

For a $10 M_{\odot}$ Schwarzschild black hole, this is approximately 220 Hz at $r = 6$.

The radial epicyclic frequency is the frequency at which a free particle oscillates about its original circular orbit if it is given a radial perturbation. In classical mechanics, the square of the radial epicyclic frequency is given by $\kappa^2 = 4\Omega^2 + r\partial\Omega^2/\partial r$, and is exactly equal to Ω^2 for Keplerian orbits in an r^{-1} potential[†] [cf. Binney & Tremaine (1987)]. In General Relativity, there is a minimum radius for which an orbit is stable to radial perturbations. The innermost marginally stable orbit is at $r = 6$ for $a = 0$, and moves inward as a increases. The epicyclic frequency is given by

$$\kappa^2 = \Omega^2 \left(1 - \frac{6}{r} + \frac{8a}{r^{3/2}} - \frac{3a^2}{r^2} \right) \quad (4.3)$$

and is zero at the marginally stable orbit. For a Schwarzschild black hole, κ reaches a maximum at $r = 8$ and is approximately 71 Hz for $M = 10 M_{\odot}$. Note that for a fixed M , the maximum κ for $a \sim 1$ is approximately equal to Ω at the marginally stable orbit for $a \sim 0$. This coincidence of time scales has led to alternative suggestions that the 300 Hz feature in GRO J1655-40 can be attributed to either the Keplerian frequency at the marginally stable orbit or to the maximum epicyclic frequency, depending upon whether one adopts $a \sim 0$ or $a \sim 1$, respectively, for this source.

Just as the radial epicyclic frequency differs from the Keplerian orbital frequency in General Relativity, so does the vertical epicyclic frequency for a spinning black hole [Kato (1990), Kato (1993), Perez, et al. (1997)]. The vertical epicyclic frequency, Ω_{\perp} , is the frequency at which a free particle oscillates about its original circular orbit if it is given a vertical perturbation. It is equal to the Keplerian orbital frequency for both Newtonian gravity and Schwarzschild black holes. In general, for non-zero black hole angular momentum it is given by:

$$\Omega_{\perp}^2 = \Omega^2 \left(1 - \frac{4a}{r^{3/2}} + \frac{3a^2}{r^2} \right) \quad (4.4)$$

As we will discuss in §5.2.3, this frequency is relevant in determining the frequencies of global ‘‘corrugation modes’’ in accretion discs [cf. Kato (1990), Kato (1993), Perez (1993), Ipser (1996)].

The final gravitational frequency that we need to consider is the Lense-Thirring precession frequency [Lense & Thirring (1918)]. If an azimuthally orbiting ring of matter is tilted out of the equatorial plane, it will begin to precess due to frame dragging effects if the black hole has non-zero angular momentum. This precession frequency, Ω_{LT} , is given by the expression:

$$\Omega_{LT} = \frac{2a}{r^3} . \quad (4.5)$$

Note that for $a \sim 1$ it is on the order of Ω , for radii near the marginally stable orbit. Furthermore, Ω_{LT} has a strong radial dependence (cf. §5.2.6).

In Figure 3 we plot these various frequencies for three angular momentum parameters, $a = 0$, $a = 0.5$, $a = 0.998$. In the inner regions of accretion discs around black holes, these frequencies typically range from $\sim 100 - 1000$ Hz, for $M = 10 M_{\odot}$, with the highest frequencies being achieved for $a \sim 1$.

[†] This is just the statement that a radial perturbation sends a circular orbit into an elliptical one, with an identical orbital period, for Newtonian free-particle orbits in an r^{-1} potential.

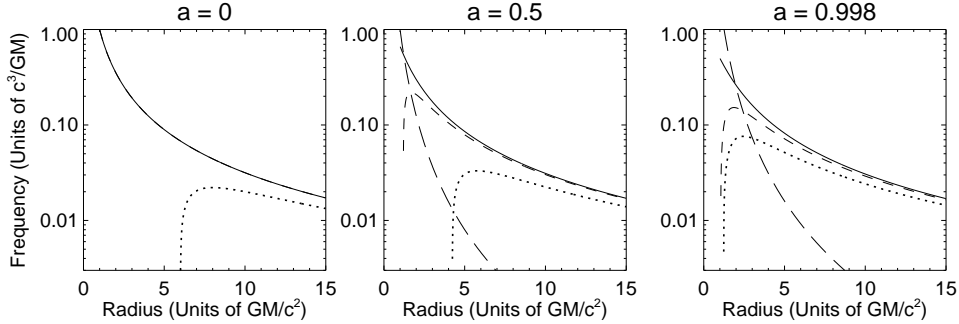


FIGURE 3. Characteristic frequencies in an accretion disc around a black hole, normalized to $c^3/GM \approx 3.2 \times 10^3$ Hz for $M = 10 M_\odot$. The angular momentum parameter, $a = cJ/GM^2$, where J is the angular momentum of the hole. Solid line is the Keplerian frequency, Ω , dotted line is the radial epicyclic frequency, κ , short dashed line is the vertical epicyclic frequency, Ω_\perp , and the long dashed line is the Lense-Thirring precession frequency, Ω_{LT} .

Note that, at least for the Schwarzschild case, the Keplerian and epicyclic frequencies can be reasonably approximated in Newtonian gravity via the use of a “pseudo-Newtonian” potential. Two such potentials that have been used in the literature are given by:

$$\Phi_{NW} = -r^{-1} \left[1 - \frac{3}{r} + \frac{12}{r^2} \right], \quad \Phi_{PW} = -r^{-1} \left[1 - \frac{2}{r} \right]^{-1}, \quad (4.6)$$

[cf. Nowak & Wagoner (1991), Paczynski & Witta (1980)]. Both of these potentials have $\kappa = 0$ at $r = 6$, and the Φ_{NW} potential has been used for Newtonian calculations of modes in relativistic discs about Schwarzschild black holes [cf. Nowak & Wagoner (1991), Nowak & Wagoner (1992), Nowak & Wagoner (1993), Nowak, et al. (1997).]

All of the above frequencies have strong radial dependences, so it is unlikely that any one of them can lead to a narrow feature at a discrete frequency without some mechanism that couples a range of radii†. Such coupling is most likely achieved via hydrodynamic effects, i.e. pressure, viscosity, etc. To this end, the most relevant *hydrodynamical* frequencies are given by the frequency of sound (for a given wavelength), ω_{cs} , and the vertical Brunt-Väisälä (i.e. buoyancy) frequency, N_z . In terms of the pressure, P , the density, ρ , and the radial and vertical perturbation wavelengths, λ_r and λ_z , these frequencies are given by:

$$\omega_{cs}^2 = c_s^2 k^2 = c_s^2 (2\pi)^2 (\lambda_r^{-2} + \lambda_z^{-2}), \quad (4.7)$$

$$N_z^2 = \left[\rho^{-2} \frac{\partial \rho}{\partial z} - (\gamma \rho P)^{-1} \frac{\partial P}{\partial z} \right] \frac{\partial P}{\partial z}. \quad (4.8)$$

For a thin disc, the sound speed is of order $h\Omega$, where h is the disc half-thickness [cf. Shakura & Sunyaev (1973)]. For radial wavelengths of $\mathcal{O}(r)$, the frequency of sound waves, $\sim (h/\lambda_r)\Omega$, is typically much less than the Keplerian frequency. The buoyancy frequency, as it deals with gradients on scales of $\mathcal{O}(h)$, can be comparable to the vertical epicyclic frequency [cf. Kato (1993)]. (Due to symmetry, however, the buoyancy

† Unless, of course, there is a “special” radius, such as the marginally stable orbit radius, which picks out a discrete frequency. However, it then may become very difficult to achieve a large luminosity modulation.

frequency vanishes at the disc mid-plane.) Both of these frequencies play a part in the theories discussed in §5.2.

5. Theoretical Models of Disc Oscillations

5.1. Historical Review

The study of oscillations relevant to accretion discs around black holes has a history that dates back more than 30 years. It was quickly realized that the α -disc model of Shakura & Sunyaev (1973) shows both viscous and thermal instabilities for high luminosities above $\mathcal{O}(10\% L_{\text{Edd}})$ [Shakura & Sunyaev (1976)]. These instabilities have often been invoked to explain the intense, broad band variability seen in BHC low/hard states[†].

As discussed in §3.1, until recently there has been little observational evidence for discrete (possibly stable) periodic modes in accretion discs about black holes. However, as was first realized by Kato & Fukue (1980), not only can accretion discs support discrete oscillatory modes, but also the effects of General Relativity modify the mode spectrum and determine the regions in which modes can be trapped. By considering adiabatic perturbations of an isothermal disc, Kato & Fukue (1980) showed that the roll-over of κ to zero at the marginally stable orbit leads to a cavity that effectively traps acoustic modes (i.e. p -modes) at the disc inner edge (cf. §5.2.1).

Later, Okazaki, et al. (1987) considered isothermal perturbations of isothermal discs and showed that it was also possible to trap what are essentially internal gravity modes (i.e. g -modes) near the epicyclic frequency maximum (cf. §5.2.2). Vishniac & Diamond (1989) considered travelling wave versions of g -modes that had an azimuthal dependence $\propto \exp[im\phi]$, with $m = 1$. These modes were invoked as a possible mechanism for angular momentum transport in an accretion disc. [Note, however, that the strictly Newtonian modes considered by Vishniac & Diamond (1989) were not trapped modes, and furthermore they had very small vertical wavelengths, i.e. $\lambda_z \ll h$.]

In a series of papers Nowak & Wagoner (1991,1992,1993) adopted a Lagrangian perturbation approach [cf. Lynden-Bell & Ostriker (1967), Freidman & Schutz (1978a,b)] to the study of disc oscillations. They showed that the acoustic modes of Kato & Fukue (1980) and Okazaki, et al. (1987) are high and low frequency limits, respectively, of the same dispersion relationship, which itself is the strong-rotation limit of the simplest form of the “helioseismology” dispersion relationship [cf. Hines (1960)]. Hence, they gave these modes the name “diskoseismology”. These works used a pseudo-Newtonian potential (eq. 4.6) to mimic the effects of General Relativity; however, they also generalized the calculations to adiabatic perturbations of non-isothermal discs. As discussed by Freidman & Schutz (1978a,b), by adopting a Lagrangian perturbation approach one can calculate a conserved (in the absence of dissipative forces) “canonical energy” for the modes[‡]. Accurately determining the canonical energy allows one to determine the effects of various dissipative effects, such as viscosity [Nowak & Wagoner (1992)], and allows one to consider various excitation mechanisms for the mode [Nowak & Wagoner (1993), Nowak, et al. (1997)]. Nowak & Wagoner (1993,1997) also considered ways in which the modes might lead to actual luminosity modulations (cf. §5.2.5).

Ipsier & Lindblom (1992) developed a scalar potential formalism for calculating modes

[†] It should be noted, however, that as shown in Fig. 1 and discussed in Nowak (1995), low/hard state luminosities are nominally below the instability limits of Shakura & Sunyaev (1976).

[‡] As Freidman & Schutz (1978a,b) point out, assigning an energy to a mode in a rotating medium is an extremely subtle issue, and many prior works were incorrect in determining this quantity.

of rotating systems in full General Relativity. Gradients of the scalar potential are related to the Lagrangian perturbation vector in both the pseudo-Newtonian formalism [Nowak & Wagoner (1992)] and the fully General Relativistic formalism [Perez, et al. (1997)]. Perez, et al. (1997) used this formalism to consider the fully relativistic version of g -modes. In addition, a third class of modes, the c -modes (cf. §5.2.3) recently have been identified and described with fully relativistic formalisms [Kato (1990), Kato (1993), Perez (1993), Ipser (1996).]

5.2. ‘Diskoseismology’

The main distinguishing feature of most of the theoretical modes described in the works cited above is that the mode frequencies predominantly depend upon fundamental gravitational frequencies and are not strongly effected by hydrodynamic processes if $h \ll r$. That is, for a thin disc, changes in density and/or pressure (which we assume to be correlated with luminosity) may effect the physical extent of a mode or its amplitude, but they do not greatly effect the mode’s frequency. Furthermore, the expected mode frequencies, $\gtrsim 100$ Hz, are comparable to the gravitational frequencies in the innermost regions of the accretion disc.

From these standpoints, the QPO features discussed in §3.1 are *not* good candidates for ‘diskoseismic’ modes. They are of very low frequency, and furthermore several, such as the 3 – 8 Hz QPO in Nova Muscae [Miyamoto, et al. (1994)], have been seen to vary in frequency by fractionally large amounts. Likewise, the low frequency ($\sim 0.1 - 10$ Hz) QPO seen in both GRS 1915+105 and GRO J1655-40 have been observed to be very highly variable in frequency [Morgan, Remillard, & Greiner (1997), Remillard, et al. (1997)].

However, the 67 Hz feature observed in GRS 1915+105 has been *consistently* observed at 67 ± 2 Hz, despite the fact that this source’s luminosity has varied by factors of two or more over the epochs during which this feature has been observed. Although there has been only one detection of the 300 Hz feature in GRO J1655-40, it was consistent with being at a steady frequency. The 300 Hz, if attributable to a disc time scale, indicates a phenomenon occurring very close to the disc inner edge. For these reasons, we identify both of these features as candidate ‘diskoseismic’ modes.

For pseudo-Newtonian potential calculations of diskoseismic modes, one defines a Lagrangian perturbation vector that describes the displacement of a fluid vector *relative to its unperturbed path* [cf. Freidman & Schutz (1978a)]. All perturbation quantities compare the *displaced*, perturbed fluid element to the (moving) fluid element in the unperturbed flow. If we take $\vec{\xi}$ to be the displacement vector, then the Lagrangian variation of the velocity, $\Delta\vec{v}$, is given by $\partial\vec{\xi}/\partial t$ [Freidman & Schutz (1978a)]. [As in Nowak & Wagoner (1991), we use Δ to denote a Lagrangian perturbation.] The Lagrangian perturbation of the density is derived from mass conservation, and is given by $\Delta\rho = -\rho\nabla\cdot\vec{\xi}$. For adiabatic oscillations, Lagrangian perturbations of the pressure are related to Lagrangian variations of the density by $\Delta P/P = \gamma\Delta\rho/\rho$, where γ is the adiabatic index [cf. Freidman & Schutz (1978a), Nowak & Wagoner (1991)].

Calculationally, it is somewhat easier to determine the mode structure by defining a scalar potential [Ipser & Lindblom (1992), Nowak & Wagoner (1992)], $\delta V(r, z) \equiv \delta P/\rho$, where here δ refers to an Eulerian perturbation†. The potential δV is seen to be the Eulerian perturbation of the enthalpy, and furthermore the Lagrangian perturbation is related to gradients of this potential [Nowak & Wagoner (1992)]. If one looks for modes

† An Eulerian perturbation is one that compares the perturbed fluid to the unperturbed fluid at a *fixed* coordinate [Freidman & Schutz (1978a)].

$\propto \exp[-i(m\phi + \sigma t)]$, where t is time and σ is the inertial mode frequency, then in a WKB approximation the modes satisfy a dispersion relationship of the form

$$[\omega^2 - \Upsilon(r)\Omega^2] (\omega^2 - \kappa^2) = \omega^2 c_s^2 k_r^2, \quad (5.9)$$

where $\omega \equiv \sigma + m\Omega$ is the corotating frequency, $\Upsilon(r)$ is a slowly varying separation function (which comes from separating the basic fluid perturbation equation into radial and vertical components), Ω and κ are the Keplerian rotation frequency and epicyclic frequency, respectively, c_s is the speed of sound, and $k_r \equiv 2\pi/\lambda_r$ is the radial wavenumber.

This dispersion relation is essentially the same as the simplest form of the helioseismology dispersion relation, except that κ takes the role of the buoyancy frequency, and $\sqrt{\Upsilon(r)}\Omega$ takes the role of the ‘acoustic cutoff’ frequency [cf. Hines (1960)]. Nowak & Wagoner (1991, 1992) showed that there are two general classes of solutions to this dispersion relation: high and low frequency. We identify the high frequency ($\omega^2 \gtrsim \kappa^2$) modes with acoustic p -modes [cf. Kato (1980), Nowak (1991), Perez (1993)], and the low frequency ($\omega^2 \lesssim \kappa^2$) modes with internal gravity g -modes [cf. Okazaki et al. (1987), Vishniac & Diamond (1989), Nowak & Wagoner (1992), Perez, et al. (1997)]. Very qualitatively, gravitational effects set certain fundamental oscillation frequencies, which are then modified by pressure effects. If the pressure forces ‘assist’ the gravitational forces, then a high frequency is achieved. If the pressure forces ‘retard’ the gravitational forces, then a low frequency is achieved. (We will return to this qualitative notion below when we consider mode excitation, cf. §5.2.4.)

The fully General Relativistic version of the diskoseismology equations leads to a WKB dispersion relationship of a very similar form. As was shown in Perez, et al. (1997), for the relativistic equations a WKB analysis still allows approximate separation of the governing equation into radial and vertical dependences. The radial component of the fluid perturbations satisfies the WKB relation

$$\frac{d^2 W}{dr^2} + \alpha^2 \left[\Psi \left(\frac{\Omega_\perp}{\omega} \right)^2 - 1 \right] (\kappa^2 - \omega^2) W = 0, \quad (5.10)$$

where $\alpha(r)$ is inversely proportional to the speed of sound at the mid-plane and $\Psi(r)$ is a slowly-varying separation function. The eigenfunction $W(r)$ is proportional to a radial derivative of the potential δV (again defined as $\delta P/\rho$) and to the radial component of the Lagrangian fluid displacement [Perez, et al. (1997)].

From the radial WKB equation (5.10) one can identify three classes of modes that are trapped. The p -modes, defined by $\Psi(\Omega_\perp/\omega)^2 < 1$, are trapped where $\omega^2 > \kappa^2$; g -modes, defined by $\Psi(\Omega_\perp/\omega)^2 > 1$, are trapped where $\omega^2 < \kappa^2$. The third class of modes (unique to the fully relativistic treatment), the c -modes, are defined by $\Psi(\Omega_\perp/\omega)^2 \cong 1$ and may in principle be trapped in either region. [The separated equation governing the vertical component involves a more complicated second-order linear operator which contains the vertical buoyancy (Brunt-Väisälä) frequency, N_z .]

The frequencies of all classes of modes are proportional to $1/M$, but their dependences on the angular momentum of the black hole are quite different. In principle this would allow one to measure the angular momentum of the black hole if more than one type of mode were to be detected in the same source. Alternatively, if one could infer the mass of the black hole through the motion of a companion which feeds the disc, such as has been done for GRO J1655-40 [Orosz & Bailyn (1997)], one could determine the angular momentum of the black hole by a single mode observation (given a correct identification for the class of mode observed). Below we briefly describe each class of mode, and we present representative examples in Figures 4–6.

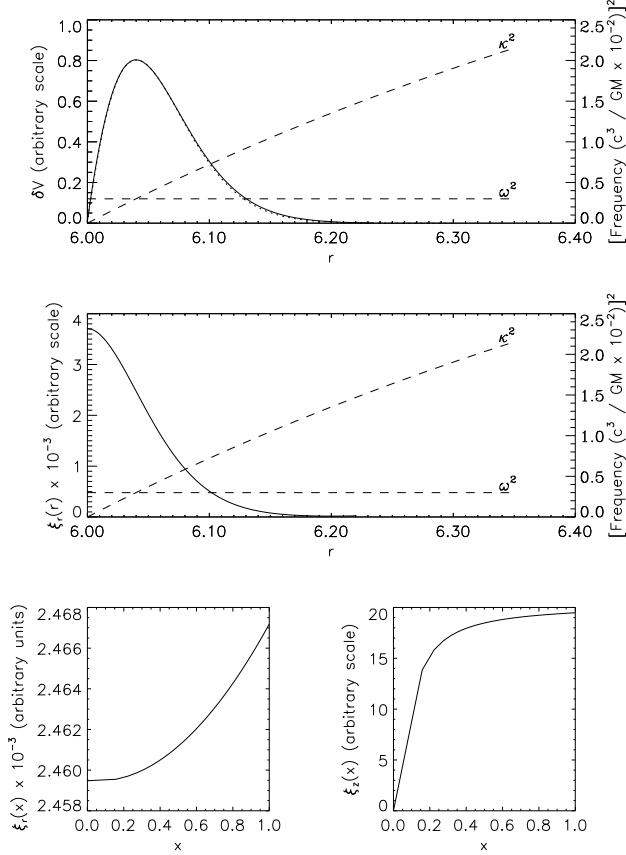


FIGURE 4. A representative $m = 0$ p -mode. Here we show the Eulerian potential, δV , as well as the radial component of the Lagrangian perturbation vector as a function of radius r , and normalized vertical coordinate, x . [Taken from Perez (1993).]

5.2.1. P -modes

As discussed by Kato (1980) and Nowak & Wagoner (1991), p -modes are trapped in regions where $\omega^2 > \kappa^2$. For $m = 0$, this leads to a narrow trapping region ($\Delta r_{\text{mode}} \ll 1$) at the disc inner edge where κ^2 goes to zero[†]. These modes have frequencies a factor of a few less than the radial epicyclic maximum, and tend to have $\xi_r \gtrsim \xi_z$ (i.e. radial perturbations greater than the vertical perturbations) [Nowak & Wagoner (1991)]. Due to their narrow confinement very near the disc inner edge [where the ‘no-torque’ disc boundary condition leads to very little luminosity modulation; Shakura & Sunyaev (1973)], we do not expect these modes to have significant luminosity modulation. We present an example of a p -mode in Fig. 4.

5.2.2. G -modes

Internal (gravity) modes are trapped where $\omega^2 < \kappa^2$, in the region where κ achieves its maximum value and where the disc is hottest. The lowest modes can have significant vertical displacements ($\xi_z \gtrsim \xi_r$) and relatively large radial extents $\Delta r \approx GM/c^2$. We believe that these modes will produce the greatest luminosity modulations in the disc;

[†] Trapped p -modes might also exist in the large, outer region of the disc; Silbergleit 1997, Private Communication.

thus, they may be the most observable class of modes [Nowak & Wagoner (1992), Perez, et al. (1997)].

To analytically approximate the eigenfunctions and eigenfrequencies of the lowest g -modes, WKB solutions to the separated radial and vertical equations of fluid perturbations can be obtained. From the symmetry of the governing equations, it is sufficient to consider eigenfrequencies $\sigma < 0$ and axial mode integers $m \geq 0$. The resulting frequencies, $f = -\sigma/2\pi$, of the lowest radial ($m = 0$) g -modes are given by

$$f = 714(1 - \epsilon_{nj})(M_{\odot}/M) F(a) \text{ Hz},$$

$$\epsilon_{nj} \approx \left(\frac{n + \frac{1}{2}}{j + \delta} \right) \frac{h}{r}. \quad (5.11)$$

Here $F(a)$ is a known, monotonically increasing function of the black hole angular momentum parameter a , with $F(a = 0) = 1$ and $F(a = 0.998) = 3.44$. The properties of the disc enter only through the small correction term ϵ_{nj} , which involves the disc thickness $2h(r)$ and the radial (n) and vertical (j) mode numbers, with $\delta \sim 1$. Typically $h/r \sim 0.1 L/L_{\text{Edd}}$ for a radiation-pressure dominated optically thick disc region, where L/L_{Edd} is the ratio of the luminosity to the Eddington (limiting) luminosity[†]. [Higher axial g -modes with $m > 0$ have a somewhat different dependence on a than the radial modes; Perez, et al. (1997)].

The 67 Hz feature observed in GRS 1915+105 has been associated with a diskoseismic g -mode [Nowak, et al. (1997)]. If this association is correct, then equation (5.11) predicts a black hole mass of $10.6 M_{\odot}$, if the hole is non-rotating, up to $36.3 M_{\odot}$, if the hole is maximally rotating. (Further aspects of this identification are discussed in §5.2.4, §5.2.5 below.) If we identify the 300-Hz feature observed in GRO J1655-40 with the fundamental g -mode oscillating in an accretion disc surrounding a $7.0 M_{\odot}$ black hole [as determined from spectra of the companion star; Orosz & Bailyn (1997)], then equation 5.11 implies that its angular momentum is 93% of maximum.

5.2.3. C -modes

To analytically obtain the approximate eigenfrequencies for the c -modes, one can solve the separated WKB perturbation equations in the regime $\Psi(\Omega_{\perp}/\omega)^2 \cong 1$ [Lehr, Wagoner, & Silbergleit (1997), Private Communication]. Here we consider c -modes that are non-radial ($m \geq 1$), nearly incompressible oscillations trapped in the very innermost region of the disc with eigenfrequencies $|\sigma| \sim m\Omega(r_c) - \Omega_{\perp}(r_c)$, where r_c is the upper radial bound of the mode. For $m = 1$ and $|a/r^{\frac{1}{2}}| \ll 1$ the fundamental c -mode eigenfrequency is approximately the Lense-Thirring frequency evaluated at the radius r_c :

$$|\sigma| \cong \frac{2a}{r_c^3}. \quad (5.12)$$

Note that for the $m = 1$ mode, r_c is typically no greater than 10% larger than the marginally stable orbit radius. The physical structure of this mode resembles a tilted inner disc which slowly precesses about the black-hole spin axis (cf. Fig 6). Since the mode is nearly incompressible, there is little temperature or pressure fluctuation in the disc, and hence a c -mode may produce very little *intrinsic* luminosity modulation (cf. 5.2.5). The mode may be observable, however, since the projected area of the inner

[†] Although the frequencies of the modes do not have a strong dependence upon L/L_{Edd} , the modes are no longer effectively trapped at large radii if $L/L_{\text{Edd}} \gtrsim 0.3$. For such high luminosities, the outer evanescent region for the g -modes becomes narrow in radius, thereby allowing g -modes to effectively couple to travelling waves in the outer regions of the disc. The modes thus “leak” energy to larger radius.

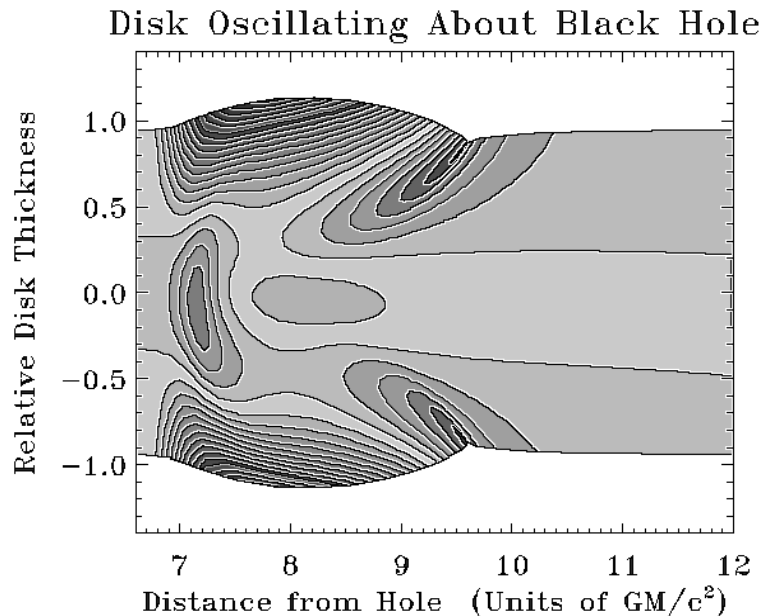


FIGURE 5. A cross section of a disc with an $m = 0$ g -mode. The disc thickness, as a function of radius, has been normalized to 1. Shaded contours correspond to the Eulerian pressure perturbations normalized to the *local* unperturbed pressure values. (The apparent asymmetry about the disc mid-plane is a numerical artifact, due to inadequate resolution of the contouring routine.)

disc changes with time. This allows the possibility of coronal emission being Compton reflected and modulated in the disc inner regions. Calculations to determine the extent of the resulting modulation are currently being undertaken [Nowak & Reynolds (1997), Private Communication].

Note that GRO J1655-40 does have a high inclination, $\sim 70^\circ$, to our line of sight [Orosz & Bailyn (1997)] making this a potentially promising mechanism for producing the observed 300 Hz feature. (Also, Compton reflection features would peak near ~ 30 keV, which is also consistent with the observations.) If we associate the 300 Hz feature with a c -mode in a disc about a $7 M_\odot$ black hole, then $a \approx 0.8$ for this source. Note that this is different from both the prediction made from assuming a g -mode in this source, as well as the prediction of Cui, et al. (1998) who associated this feature with Lense-Thirring precession at a single radius (cf. 5.2.6). In Fig. 6 we show the c -mode frequency as a function of the angular momentum parameter a .

5.2.4. Excitation and Damping Mechanisms

It is possible to use a parameterized stress tensor to estimate the effects of turbulent viscosity on the g -modes [Nowak & Wagoner (1992,1993)]. The canonical energy of a radial mode is $E_c \sim \sigma^2 \rho (\xi_z^2 + \xi_r^2) dV$, where here dV is the volume occupied by the mode. Isotropic turbulence produces a rate of change $dE_c/dt \equiv -E_c/\tau$, with $\tau \sim |\alpha \sigma [h^2/\lambda_r^2 + h^2/\lambda_z^2]|^{-1}$. Here λ_r and λ_z , respectively, are the radial and vertical mode wavelengths, and α is the standard Shakura-Sunyaev α -parameter [Shakura & Sunyaev (1973)]. The corresponding quality factor is given by

$$Q_{jn}^{-1} = (|\sigma|\tau)^{-1} \sim [j^2 + (h/r)n^2] \alpha, \quad (5.13)$$

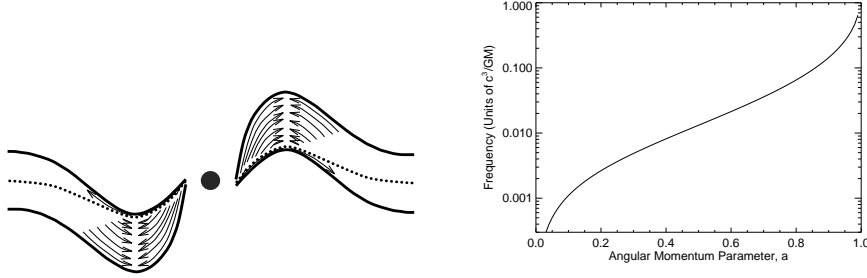


FIGURE 6. *Left:* Schematic drawing of a c -mode in an accretion disc (arbitrary amplitude). *Right:* Frequencies of the fundamental $m = 1$ c -mode frequency as a function of the black hole angular momentum parameter $a \equiv cJ/GM^2$. Frequencies are normalized to $c^3/GM \approx 3.2 \times 10^3$ Hz for $M = 10 M_\odot$.

as $\lambda_z \sim h/j$ and $\lambda_r \sim \sqrt{hr}/n$, where j and n are of order of the number of vertical and radial nodes in any particular eigenfunction. Thus, for $\alpha \ll 1$, we can have high mode Q [cf. Nowak & Wagoner (1993); Nowak, et al. (1997)].

The above estimates are for *isotropic* viscosity. If the turbulence does not efficiently couple to the vertical gradients of the modes, then the mode Q value is increased by a factor $\sim (j\lambda_r/h)^2$ [cf. Nowak & Wagoner (1993)]. Aside from damping modes, turbulence can also potentially excite modes. Velocity perturbations in the disc, $\delta\vec{v}$, are made up of a mode component, $\delta\vec{v}_M$, and a turbulent component, $\delta\vec{v}_T$. Viscous damping arises from terms of the form $\delta v_{Mi}\delta v_{Tj}$, while mode excitation arises from terms of the form $\delta v_{Ti}\delta v_{Tj}$ [Nowak & Wagoner (1993)]. It is possible to make simple estimates of the magnitude of the turbulent excitation, and balance this against the turbulent damping [Nowak & Wagoner (1993)]. The modes are excited to an amplitude of $|\xi^z| \sim \alpha(h/\lambda_r)^{3/2} h$, and $\sim \alpha\sqrt{\lambda_r/h} h$, for isotropic and anisotropic viscosity, respectively [Nowak & Wagoner (1993)]. If turbulence is playing the dominant role in damping and exciting the modes, then we have the following constraints. For isotropic turbulence, the Q value is large only for $\alpha \ll 1$; however, this implies a correspondingly small amplitude. For anisotropic viscosity, a larger mode amplitude and a higher Q is achieved for a given α . However, in either case it is likely very difficult to achieve amplitudes as large as required to agree with the observations of GRS 1915+105 and GRO J1655-40 (cf. §5.2.5).

Another potential excitation mechanism for g -modes is ‘negative radiation’ damping [Nowak, et al. (1997)]. As a first approximation, the g -modes are taken to be adiabatic. In reality, one expects there to be small entropy changes due to various effects, the most notable one being radiative losses. If one has a radiation pressure dominated atmosphere, as is likely in high-luminosity discs, one properly should use

$$\Delta P = \gamma \frac{P}{\rho} \Delta \rho + \gamma \frac{P}{s} \Delta s, \quad (5.14)$$

where s is the specific entropy. The effects of this term for a radiation pressure dominated atmosphere can be approximated by writing an ‘effective’ adiabatic index, γ' , to be substituted into the relationship between the Lagrangian variations of the pressure and density. Nowak, et al. (1997) showed this term to be

$$\gamma' \approx \gamma \left(1 + i \frac{\gamma c}{4\omega\tau_{es}h} \right) \equiv \gamma(1 + i\alpha') , \quad (5.15)$$

where τ_{es} is the scattering depth of the disc and h is the disc half thickness. In the

above, our ignorance of the disc's true vertical structure is subsumed into the parameter α' , which one expects to be of $\mathcal{O}(\alpha)$ for a radiation pressure-dominated disc.

It is the imaginary component of the effective adiabatic index that leads to radiative damping for p -modes but conversely leads to excitation of the g -modes. One can see this by perturbing the approximate dispersion relationship $\omega^2 \approx \kappa^2 \pm c_s^2 k_r^2$, where the $+$ is for p -modes and the $-$ is for g -modes. Perturbing the frequency and the sound speed together, we have:

$$\delta\omega\omega \approx \pm \delta c_s c_s k_r^2, \quad (5.16)$$

where $\delta c_s^2 \sim i\alpha' c_s^2$. Thus, the imaginary component of γ' leads to damping of p -modes and excitation of g -modes. Qualitatively, as the p -mode compresses gas, radiation leaks out, thereby providing less restoring force from the compressed region, and therefore leads to damping. As discussed above, the g -mode is in some sense opposite as the pressure works *against* the gravity. Hence, radiative leaking leads to less effective pressure restoring forces and thereby to g -mode growth.

5.2.5. Luminosity Modulation

For most simple α -models, the energy generation rate per unit volume in the accretion disc is approximated by $\alpha P(r, z)\Omega(r)$. The local pressure is modulated by p - and g -modes (and to a much lesser extent by c -modes); thus, there is the possibility that these modes can lead to an observable luminosity modulation. Furthermore, the modes not only perturb the pressure, but they also perturb the locations of the disc boundaries. As discussed in Nowak, et al. (1997), the integrated variation of the energy generation rate is therefore

$$\begin{aligned} \delta L \sim 2\pi \left[\int_{r_I + \xi_r(r_I)}^{r_O + \xi_r(r_O)} r' dr' \int_{-z_0 + \xi_z(-z_0)}^{z_0 + \xi_z(z_0)} \alpha \Omega P'(r', z') dz' \right. \\ \left. - \int_{r_I}^{r_O} r dr \int_{-z_0}^{z_0} \alpha \Omega P(r, z) dz \right], \quad (5.17) \end{aligned}$$

where $P'(r', z') \equiv P(r, z) + \Delta P(r, z)$, $r' \equiv r + \xi_r(r)$, $z' = z + \xi_z(z)$, and r_I , r_O , z_0 are the disc boundaries (r_O can be taken to go to ∞ without loss of generality).

The g -modes have the most promising combination of pressure modulation and physical extent, which makes them the most likely candidates to be observed by direct luminosity modulation of this sort. However, for standard disc models, only a few percent of the total luminosity is generated in the region of the disc where the g -modes can exist. Thus, we expect only of $\mathcal{O}(1\%)$ rms modulation due to the g -modes. This is consistent with the observations of GRS 1915+105 and GRO J1655-40; however, as shown in Nowak, et al. (1997), even this modest luminosity modulation requires large mode amplitudes. Specifically, $\xi_z \sim h$ is required[†].

Qualitatively, as the g -modes exist in the inner, hotter disc regions, one expects the modulated luminosity to be harder than the average *disc* luminosity. However, both the 67 Hz and 300 Hz QPO seem to be strongest in the *power law tail*, which is problematic for the g -mode interpretation of these modes if one associates the power law tail with a corona distinct from the accretion disc.

On the other hand, although one expects the c -modes to have relatively little luminosity modulation due to pressure fluctuations, these modes may be effective at modulating

[†] Note, however, that Nowak, et al. (1997) only considered Schwarzschild black holes. As a disc about a Kerr black hole releases a fractionally greater amount of its energy in the g -mode region, one may only require a mode amplitude a factor of several smaller.

reflected emission. If the power law tail is due to a corona above a cold accretion disc, then part of this power law will be Compton reflected [Magdziarz & Zdziarski (1995)], and hence may be modulated by the warping associated with the c -modes. Furthermore, one expects the reflected emission to peak in the 20 – 30 keV range [Magdziarz & Zdziarski (1995)], which is consistent with the observations of both GRS 1915+105 and GRO J1655-40.

5.2.6. *Alternative Models*

The diskoseismology g -mode interpretation of the 67 Hz and 300 Hz has several points in its favor. First, it reproduces the correct time scales. Second, the g -mode frequencies, like the observed 67 Hz frequency, are expected to be relatively insensitive to luminosity fluctuations. Third, mode Q of $\mathcal{O}(20)$ is achievable with a reasonable α -parameter. Fourth, there is an identified mechanism (negative radiation damping) for exciting the modes. Fifth, the g -modes are capable of modulating the luminosity of the disc, possibly as much as the observed $\sim 1\%$. Furthermore, we qualitatively expect the modes to be harder than the mean disc spectrum.

There are two major arguments against the g -mode interpretation. First, one requires a large mode amplitude (although this might be reduced slightly if one considers near maximal Kerr holes). Second, the observed QPO features appear strongest in the power law tails, which are not necessarily associated with a disc component. Aside from the c -modes discussed above, there are several other alternative hypotheses to the g -modes.

One possibility is fluctuations in the location of the sonic point [Honma, Matsumoto, & Kato (1992)], which can lie just inside of the marginally stable orbit, where disc orbits are going from circular orbits to near free-fall trajectories. As discussed by Honma, Matsumoto, & Kato (1992), the time scales associated with this ‘pulsational instability’ of the sonic point are fairly rapid. Again, one needs to show that sufficient luminosity modulation is possible with such a mechanism.

Milsom & Taam (1997) have numerically shown that for some accretion disc models, one finds acoustic p -modes that, although not trapped, peak at the location of the epicyclic frequency maximum[†]. Furthermore, their frequency is that of the epicyclic frequency maximum. Many predictions of the p -mode hypothesis, such as the mass and angular momentum of the central object, are identical to those made by the g -mode hypothesis. As for the g -modes, it is also difficult to achieve $\mathcal{O}(1\%)$ luminosity modulation, and likewise it may also be difficult to produce features as hard as those observed in GRS 1915+105 and GRO J1655-40.

More recently, Cui, Zhang, & Chen (1998) have proposed that the observed QPO features are associated with Lense-Thirring precession. Specifically, these authors choose the QPO frequency to be the Lense-Thirring frequency at the radius at which the accretion disc effective temperature is maximum, and thus derive $a \sim 1$ for both GRS 1915+105 and GRO J1655-40. There are a number of objections to this picture. First, choosing the radius to be that of the effective temperature maximum is somewhat arbitrary, and one might expect that the radius at which $r^2 F_\gamma$ is maximized, where F_γ is the disc photon flux over the observed energy bands, is a more natural choice. Second, neither F_γ nor $r^2 F_\gamma$ are sharply peaked functions, therefore it is extremely unlikely that one can generate a feature with $Q \sim 20$, as was observed for the 67 Hz feature in GRS 1915+105. [From this point of view, the c -modes discussed in §5.2.3 are the natural, ‘global’ features to be

[†] Qualitatively, one can understand this by considering the p -mode dispersion relationship, which is $(\omega^2 - \kappa^2) \approx c_s^2 k^2$. The p -mode group velocity is seen to go to zero at $\omega^2 = \kappa^2$. Thus p -modes with the maximum epicyclic frequency “stall” at the location of the epicyclic frequency maximum.

associated with Lense-Thirring precession.] Third, due to frame dragging effects in the presence of viscous forces, one expects that the inner region of the disc will be flattened and constrained to the equatorial plane on a time scale of $\mathcal{O}(1\text{s})$ [Bardeen & Petterson (1975)][‡]. Fourth, Cui, Zhang, & Chen (1998) do not identify any luminosity modulation mechanism. Finally, Cui, Zhang, & Chen (1998) do not demonstrate that there is a viable excitation mechanism for the modes [although they suggest that the radiative warping mechanism of Pringle (1996) may be at work]. However, as discussed above, the c -modes, which are qualitatively similar to the Lense-Thirring precession suggested by Cui, Zhang, & Chen (1998), may yet provide a viable explanation for the observed high frequency QPO features.

6. Summary

As was discussed in §5.1, the study of stable oscillations in accretion discs has a long and rich history. However, it was not until the advent of *Ginga* in the late 1980's and of *RXTE* in only the past few years that this field has also become an observational one.

Prior to the launch of *RXTE*, there were only a few observations of QPO features in BHC. Most of these features were of low frequency $\lesssim 10$ Hz (this was likely mainly due to instrumental limitations), were not seen during more than one epoch, and were often broad ($Q \lesssim 10$) and often variable in frequency. Few theories have been put forth that adequately describe these observations.

In the past two years since the launch of *RXTE*, a wealth of new observational information has been obtained. Again, a number of low-frequency, often broad and highly variable features have been observed. Among the wealth of features seen with *RXTE*, two high frequency features stand out: the 67 Hz feature in GRS 1915+105 and the 300 Hz feature in GRO J1655-40. The former is notable for its steady frequency, whereas the latter is notable for its high frequency which suggests very strongly that it comes from very close to the probable $7 M_{\odot}$ black hole in this system.

The high frequency of both features and the stability of the 67 Hz feature suggests that these QPO might be related to stable oscillations in the inner regions of accretion discs. We have described a class of theories, which we refer to as ‘diskoseismology’, that might offer an explanation for these observations. The main motivations for attributing these features to diskoseismic modes are that these modes: 1) are related to a ‘natural’ frequency in the disc (i.e. the maximum epicyclic frequency); 2) their spectra are expected to be characteristic of the inner, hottest regions of the disc; 3) their frequencies are relatively insensitive to changes in luminosity; and 4) they have low rms variability.

This latter feature, although in agreement with the observations, is the strongest constraint. These modes *cannot* be applied to systems that show $\gtrsim 10\%$ rms variability over a wide range of energy bands. Furthermore, it may be difficult to explain the observed spectral hardness of the QPO. To these ends, one needs to begin to consider more detailed *dynamical* disc models that address the production of the hard radiation. Also, g -modes have been the major focus of recent study; however, c -modes, which are related to Lense-Thirring precession of warped accretion discs, may offer a better expla-

[‡] Cui, Zhang, & Chen (1998) mistakenly claimed that this time scale was very long; however, they were quoting the time scale for the black hole’s angular momentum to align with the binary orbital angular momentum (which is of order millions of years). The time scale for the inner region of the disc to flatten into the orbital plane is significantly shorter. Note that the c -modes should also be susceptible to damping by the ‘Bardeen-Petterson’ effect; however, as they are global modes we expect the damping time scale to be slightly longer than that suggested by Bardeen & Petterson (1975).

nation of some of the data. Finally, in all of the above work magnetic fields have been neglected. As shown by Balbus & Hawley (1992), even weak magnetic fields can play an important dynamical role. The incorporation of magnetic fields into the diskoseismology calculations is one of the next major steps that needs to be addressed.

Even if the features seen in GRS 1915+105 and GRO J1655-40 do not turn out to be diskoseismic modes, they point out two important lessons. First, BHC systems can produce relatively stable, high-frequency features. Second, the *Rossi X-ray Timing Explorer* is capable of detecting and characterizing these features despite their weak variability. In a very real sense, despite nearly twenty years of research, the study of stable oscillations in black hole accretion systems has just begun.

The authors would like to acknowledge useful conversations with Robert Wagoner, Mitchell Begelman, Brian Vaughan, Chris Perez, Ron Remillard, and Ed Morgan. M.A.N. was supported in part by an LTSA grant from NASA (NAG 5-3225). D.E.L. was supported in part by a NASA GSRP Training Grant NGT5-50044.

REFERENCES

- BALBUS, S. A., & HAWLEY, J. F. 1992 A powerful local shear instability in weakly magnetized disks. I - Linear analysis. II - Nonlinear evolution. *Ap. J.* **376** 214–233.
- BARDEEN, J. M., & PETERSON, J. A. 1975 *Ap. J.* **195** L65.
- BINNEY, J., & TREMAINE, S. 1987 *Galactic Dynamics*. Princeton Press.
- CHEN, X., SWANK, J. H., TAAM, R. E. 1997 The pattern of correlated X-ray timing and spectral behavior in GRS 1915+105. *Ap. J.* **477** L41–L44.
- CUI, W., ZHANG, S. N., FOCKE, W., & SWANK, J. H. 1997 Temporal properties of Cygnus X-1 during the spectral transitions. *Ap. J.* **484** 383–393.
- CUI, W., ZHANG, S. N., & CHEN, W. 1998 Evidence for frame dragging around spinning black holes in X-ray binaries. *Ap. J.* **492** L53–L57.
- DAVENPORT, W. B., JR., & ROOT, W. L. 1987 *An Introduction to the Theory of Random Signals and Noise*. IEEE Press.
- EBISAWA, K., MITSUDA, K., & INOUE, H. 1989 Discovery of 0.08-Hz quasi-periodic oscillations from the black hole candidate LMC X-1. *P. A. S. J.* **41**, 519–530.
- FRIEDMAN, J. L., & SCHUTZ, B. F. 1978 Lagrangian perturbation theory of nonrelativistic fluids. *Ap. J.* **221** 937–957.
- FRIEDMAN, J. L., & SCHUTZ, B. F. 1978 Secular Instability of rotating newtonian stars. *Ap. J.* **222** 281–296.
- GREBENEV, S. A., SYUNYAEV, R. A., PAVLINSKII, M. N., & DEKHANDOV, I. A. 1991 Detection of quasiperiodic oscillations of X-rays from the black-hole candidate GX 339-4. *Sov. Astron. Lett.* **17**, 413–415.
- HINES, C. O. 1960 *Can. J. Phys.* **38** 1441.
- HJELLMING, R. M., & RUPEN, M. P. 1995 Episodic ejection of jets by the X-ray transient GRO:J1655-40. *Nature* **375** 464.
- HONMA, F., MATSUMOTO, R., & KATO, S. 1992 Pulsational instability of relativistic accretion disks and its connection to the periodic X-ray time variability of NGC 6814. 1992 *P. A. S. J.* **44** 529–535.
- IPSER, J. R., & LINDBLOM, L. 1992 On the pulsations of relativistic accretion disks and rotating stars - the Cowling approximation. *Ap. J.* **389** 392–399.
- IPSER, J. R. 1996 Relativistic accretion disks: low-frequency modes and frame dragging. *Ap. J.* **458** 508–513.
- IWASAWA, K., FABIAN, A. C., BRANDT, W. N., KUNIEDA, K., MISAKI, K., REYNOLDS, C. S., & TERASHIMA, Y. 1998 Detection of an X-ray periodicity in the Seyfert galaxy IRAS18325-5926. *M. N. R. A. S.*, in Press.

- KATO, S., & FUKUE, J. 1980 Trapped radial oscillations of gaseous disks around a black hole. *P. A. S. J.* **32** 377–388.
- KATO, S. 1990 Trapped one-armed corrugation waves and QPOs. *P. A. S. J.* **42** 99–113.
- KATO, S. 1993 Amplification of one-armed corrugation waves in geometrically thin relativistic accretion disks. *P. A. S. J.* **45** 219–231.
- KITAMOTO, S., TSUNEMI, H., MIYAMOTO, S., & HAYASHIDA, K. 1992 Discovery and X-ray properties of GS 1124–683 (=Nova Muscae). *Ap. J.* **394**, 609–614.
- KOUVELIOTOU, C., FINGER, M. H., FISHMAN, G. J., MEEGAN, C. A., WILSON, R. B., PACIESAS, W. S. 1992a *I. A. U. Circ.* 5576.
- _____. 1992b *I. A. U. Circ.* 5592.
- LENSE, J. & THIRRING, H. 1918 *Phys. Z.* **19** 156.
- LYNDEN-BELL, D. & OSTRICKER, J. P. 1967 On the stability of differentially rotating bodies. *M. N. R. A. S.* **136** 293–310.
- MAGDZIARZ, P. AND ZDZIARSKI, A. 1995 Angle-Dependent Compton reflection of X-rays and gamma-rays. *M. N. R. A. S.* **273** 837–848.
- MILSON, J. A., & TAAM, R. E. 1997 Two-dimensional studies of inertial-acoustic oscillations in black hole accretion discs. *M. N. R. A. S.* **286** 358–368.
- MIRABEL, & RODRIGUEZ, 1994 A superluminal source in the galaxy. *Nature* **371** 46.
- MIYAMOTO, S., KIMURA, K., KITAMOTO, S., DOTANI, T., & EBISAWA, K. 1991 X-ray variability of GX 339–4 in its very high state. *Ap. J.* **383** 784–807.
- MIYAMOTO, S., KITAMOTO, S., IGA, S., NEGORO, H., & TERADA, K. 1992 Canonical time variations of X-rays from black hole candidates in the low-intensity state. *Ap. J.* **391** L21–L24.
- MIYAMOTO, S., IGA, S., KITAMOTO, S., & KAMADO, Y. 1993 Another canonical time variation of X-rays from black hole candidates in the very high flare state? *Ap. J.* **403** L39–L42.
- MIYAMOTO, S., KITAMOTO, S., IGA, S., & HAYASHIDA, K. 1994 Normalized power spectral densities of two X-ray components from GS 1124–683. *Ap. J.* **435** 398–406.
- MORGAN, E. H., REMILLARD, R. H., & GREINER, J. 1997 RXTE observations of QPOs in the black hole candidate GRS 1915+105. *Ap. J.* **482** 993–1010.
- NOWAK, M. A. 1995 Towards a unified view of black hole high energy states. *P. A. S. P.* **718** 1207–1216.
- NOWAK, M. A., & WAGONER, R. V. 1991 Diskoseismology: probing accretion disks I. Trapped adiabatic oscillations. *Ap. J.* **378** 656–664.
- NOWAK, M. A., & WAGONER, R. V. 1992 Diskoseismology: probing accretion disks II. G-modes, gravitational radiation reaction, and viscosity. *Ap. J.* **393** 697–707.
- NOWAK, M. A., & WAGONER, R. V. 1993 Turbulent generation of trapped oscillations in black hole accretion disks. *Ap. J.* **418** 187–201.
- NOWAK, M. A., WAGONER, R. V., BEGELMAN, M. C., & LEHR, D. E. 1997 The 67 Hz feature in the black hole candidate GRS 1915+105 as a possible “diskoseismic” mode. *Ap. J.* **477** L91–L94.
- OKAZAKI, A., KATO, S., & FUKUE, J. 1987 Global trapped oscillations of relativistic accretion disks. *P. A. S. J.* **39** 457–473.
- OROSZ, J. A., & BAILYN, C. D. 1997 Optical observations of GRO J1655-40 in quiescence. I. A precise mass for the black hole primary. *Ap. J.* **477** 876–896.
- PAZCZYNSKI, B. & WITTA, P. 1980 *A. & A.* **88** 23.
- PEREZ, C. A. 1993 *Ph.D. Thesis, Dept. of Physics, Stanford University.*
- PEREZ, C. A., SILBERGLEIT, A. S., WAGONER, R. V., & LEHR, D. E. 1997 Relativistic diskoseismology. I. Analytical results for “gravity modes”. **476** 589–604.
- PRESS, W. H., TEUKOLSKY, S. A., VETTERLING, W. T., & FLANNERY, B. P. 1992 *Numerical Recipes in FORTRAN. The Art of Scientific Computing, 2nd Edition.* Cambridge Press.
- PRINGLE, J. E. 1996 *M. N. R. A. S.* **281** 357–361.

- REMILLARD, R. A., MORGAN, E. H., MCCLINTOCK, J. E., BAILYN, C. D., OROSZ, J. A., & GREINER, J. 1997 In *Proceedings of the 18th Texas Symposium on Relativistic Astrophysics* (eds. A. Olinto, J. Frieman, & D. Schramm) Univ. Chicago Press.
- SHAKURA, N. I., & SUNYAEV, R. A. 1973 Black holes in binary systems. observational appearance. *A. & A.* **24** 337–355.
- SHAKURA, N. I., & SUNYAEV, R. A. 1976 A theory of the instability of disk accretion on to black holes and the variability of binary X-ray sources, galactic nuclei, and quasars. *M. N. R. A. S.* **175** 613–632.
- SUNYAEV, R. A., CHURAZOV, E., GILFANOV, M., NOVIKOV, B., GOLDWURM, A., PAUL, J., MANDROU, P., & TECHINE, P. 1992 *I. A. U. Circ.* 5593.
- SUNYAEV, R. A., ET AL. 1993 Broad-band X-ray observations of the GRO J0422+32 X-ray nova by the “Mir-Kivant” observatory. *A. & A.* **280** L1–L4.
- TAAM, R. E., CHEN, X., SWANK, J. H. 1997 Rapid bursts from GRS 1915+105 with RXTE. *Ap. J.* **485** L83–L86.
- TANAKA, Y., AND LEWIN, W. H. G. 1995, Black hole binaries. In *X-ray Binaries* (eds. W. H. G. Lewin, J. van Paradijs, & E. P. J. van den Heuvel), Cambridge University Press.
- UBERTINI, P., BAZZANO, A., COCCHI, M., LA PADULA, C., POLCARO, V. F., STAUBERT, R., KENDZIORRA, E. 1994 Hard X-ray timing observation of the Crab pulsar and Cygnus X-1. *Ap. J.* **421** 269–275.
- VAN DER KLIS, M. 1994 Similarities in neutron star and black hole accretion. *Ap. J. S.* **92** 511–519.
- _____. 1995 Rapid aperiodic variability in X-ray binaries. In *X-ray Binaries* (eds. W. H. G. Lewin, J. van Paradijs, & E. P. J. van den Heuvel), Cambridge University Press.
- VIKHLININ, A., ET AL. 1994 Discovery of a low-frequency broad quasi-periodic oscillation peak in the power density spectrum of Cygnus X-1 with Granat/SIGMA. *Ap. J.* **424** 395–400.
- VISHNIAC, E. T., & DIAMOND, P. 1989 A self-consistent model of mass and angular momentum transport in accretion disks. *Ap. J.* **347** 435–447.